Characterization of Electrosprays and Its Relevance to Colloid Thrusters.

Manuel Gamero-Castaño & Vladimir Hruby
Busek Co. Inc.
11 Tech Circle
Natick, MA 01760-1023
busek@busek.com
508-655-5565

IEPC-01-283

In this article we use a combination of energy analysis and time of flight techniques to measure a set of electrofluiddynamic parameters that are relevant to electrosprays in the cone-jet mode. Knowledge of the voltage difference between electrospraying needle and the point at which charged droplets are formed, the initial velocity of the droplets and their specific charge distribution function, is essential to comprehend properties of the Colloid thruster such as its thrusting efficiency. We find that a large fraction of the electrospray needle voltage is used to accelerate the jet, and the pressure of the jet's fluid at the breakup point is negligible as compared to its specific kinetic energy. We expect that these measurements will guide the analytical modeling of cone-jets, which is necessary to understand the performance of Colloid thrusters.

I. Introduction.

The research on the suitability of electrospray for space propulsion dates back to the early 60's[1,2] and continuous effort extended well into the next decade[3]. The colloid source most commonly used during this stage consisted of multi-jet, highly stressed electrosprays of glycerol. Because of the relatively poor conductivity of glycerol (see reference [4], where a 19.3% solution by weight of NaI in glycerol has an electrical conductivity of 0.021 S/m), very high onset voltages were required to obtain colloid beams with reasonable specific impulses (values of 10 kV were typical). Even though successful lab prototypes were eventually built,[5] interest in this technology decreased and eventually disappeared. An extended review of the early effort in this field is given in reference [6].

Several reasons have recently rekindled the interest in colloid thruster technology: first, the low output thrust typical of a single electrospray is now seen as an advantage rather than a problem, and is in fact essential in some missions as interest has increased for propulsion capability for smaller spacecraft. Second, the need for formation flying of multiple satellites whose relative positions must be precisely controlled calls for a propulsive scheme characterized by continuous microthrust levels, which also must offer the possibility of fine thrust variations. Only colloid and field emission (FEEP) thrusters are thought to yield this performance. Third, the knowledge gained during the last decade in the electrospraying of liquids allows now a reasonable understanding of the colloid generation. Use of more conducting solvents than glycerol enables the generation of sprays with the desired high specific impulse in the single cone-jet mode at

Presented as Paper IEPC-01-283 the 27th International Electric Propulsion Conference, Pasadena, CA, 15-19 October, 2001

onset voltages (~1.5 kV) much lower than previously. Furthermore, this new knowledge allows a confident design of the colloid source based on physical laws.

A photograph of an electrospray held in vacuum is shown in Figure 1. A given liquid flow rate is fed through a capillary, metallic needle, and a voltage difference between needle and a facing electrode (not seen in Figure 1) is set. If the voltage and flow rate are adequate, a stable liquid meniscus with a slender jet issuing from its apex is formed. Eventually, the jet becomes unstable and breaks up, generating a spray of charged droplets. Because of the geometric resemblance, the type of electrospray depicted in Figure 1 is commonly known as cone-jet mode.[7]

In a previous article we studied the suitability of cone-jets as a source of charged particles for space propulsion, as well as the properties of several propellant candidates.[8] This paper will focus on measuring and interpreting characteristics of the electrospray such as the voltage drop along the cone-jet, the velocity of the jet at the breakup location, and the specific charge of electrospray droplets. These quantities are measured using time of flight and retarding potential techniques. A more detailed account can be found in reference [9].

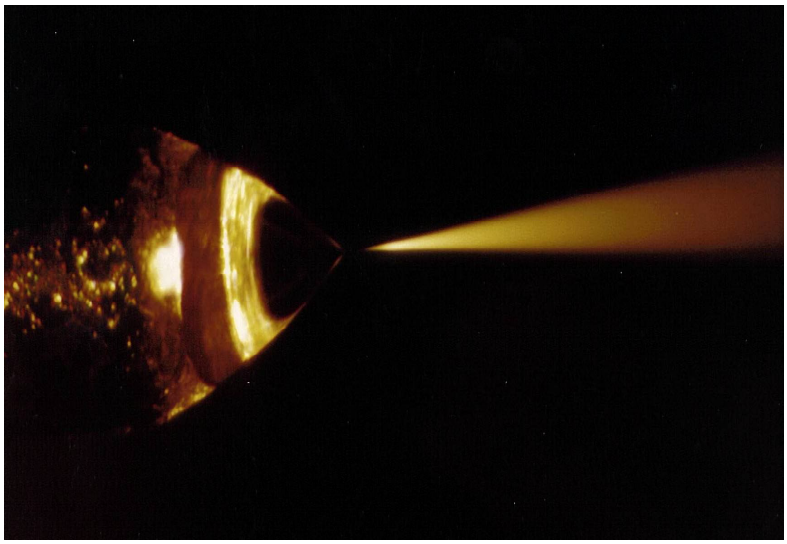

Figure 1 Electrospray of TBP held in vacuum (taken from reference [10])

II. Experimental

We have studied five solutions of tributyl phosphate, TBP, with electrical conductivities ranging from 2.3×10^{-4} S m^{-1} to 2.2×10^{-2} S m^{-1}. Table 1 lists the name of each solution, solute concentrations and conductivities. The ionic liquid 1-ethyl-3-methylimidazolium bis (trifluoromethylsulfonyl) imide, was used for enhancing the conductivity of TBP1, while tetrabutylammonium tetraphenyl borate was added to the remaining solutions. The surface tension, density, dielectric constant and viscosity coefficient of pure TBP are $\gamma = 0.028$ N m^{-1}, $\rho = 976$ kg m^{-3}, $\varepsilon = 8.91$ and $\mu = 0.00359$ Pa s^{-1} respectively.[11] We will assume that the modest solute concentrations of the solutions in Table 1 do not affect significantly the physical properties of TBP.

Figure 2 shows the schematics of the vacuum facility and electrospray source employed in these experiments. The electrospray source is mounted inside a 5 cm diameter cross (electrospray chamber), joined to a 1x1.3 m cylindrical tank (vacuum tank). The electrodes used to analyze the sprays are installed in this larger chamber. A 25 cm diffusion pump backed by a mechanical pump evacuates the system down to 10^{-3} Pa. The design of the electrospray source is simple: a plastic reservoir contains the TBP solution, which is fed to the electrospray needle through a fused silica capillary.

The liquid flow rate is varied by changing the pressure inside the solution reservoir, and measured by means of a bubble flowmeter connected in series to the fused silica line. The electrospray needle is also a fused silica capillary, with one of its ends connected to the flowmeter while the other is shaped into a cone (needle tip) and made electrically conductive by depositing a layer of tin oxide on its surface. An extractor electrode with a small orifice faces the needle tip. The distance between the tip of the needle and the facing extractor is approximately 2.5 mm. The diameter of the extractor's orifice is roughly 0.8 mm. In order to form a cone-jet, the TBP solution is fed to the needle and an appropriate voltage difference between needle and extractor (typically 1600 V), is set. The beam of droplets exits the needle-extractor region through the extractor orifice, and enters the large vacuum tank where it is subsequently analyzed.

Table 1 Compositions and electrical conductivity of the solutions electrosprayed.

Solution	Solute	Solute concentr.	K (S m^{-1})
TBP1	Emi-Im*	2.9%w	2.20 $x10^{-2}$
TBP2	TBTP**	1.5%w	8.53 $x10^{-3}$
TBP3	TBTP	0.15%w	1.64 $x10^{-3}$
TBP4	TBTP	0.050%w	5.34 $x10^{-4}$
TBP5	TBTP	0.015%w	2.30 $x10^{-4}$

*1-ethyl-3-methylimidazolium bis (trifluoromethylsulfonyl)imide
**tetrabutylammonium tetraphenyl borate

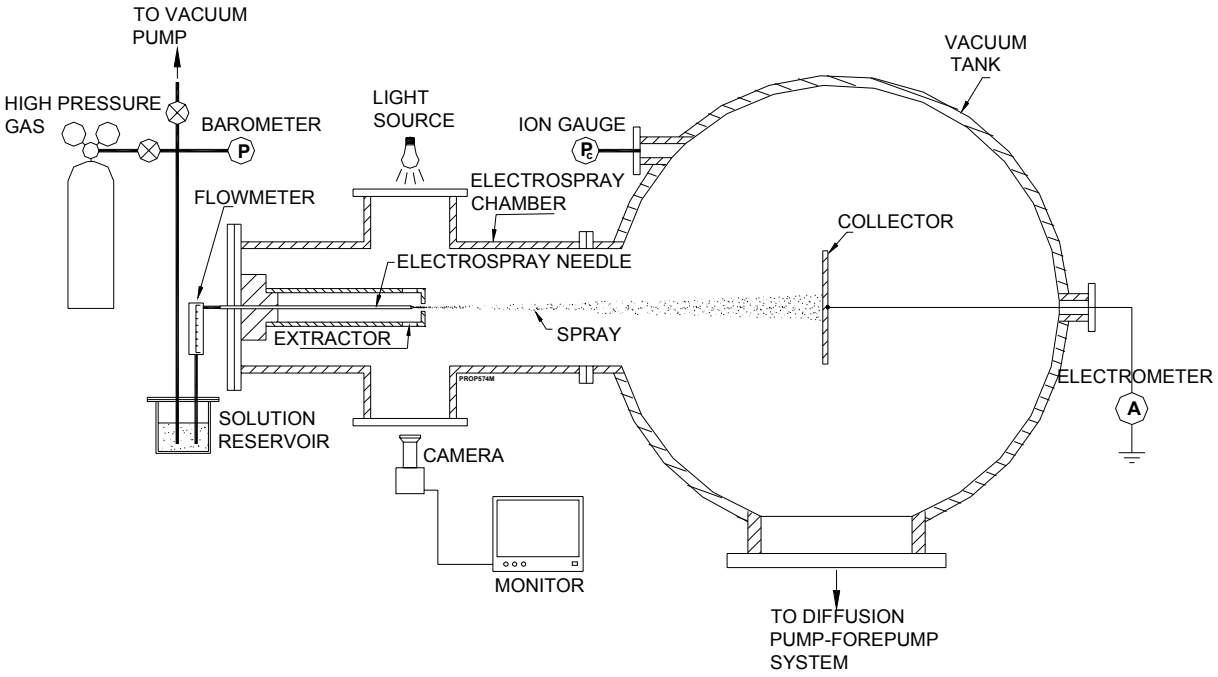

Figure 2 Sketch of the electrospray source and vacuum facility.

A detailed description of the additional arrangement (collector electrodes where the current of the beam is measured, power supplies, electronics, connections, etc.) required for performing stopping potential and time of flight measurements of the electrospray beam was given elsewhere.[8,12]

III. Results and discussion.

Figure 3 shows the stopping potential curve associated with an electrospray of solution TBP3. The flow rate and electric current of this spray are 6.5×10^{-12} m^3 s^{-1} and 47 nA. We plot the electric current measured at a grounded collector facing the beam, approximately 5 cm from the extractor (the collector is located inside the large vacuum tank), as a function of the electrospray needle voltage referred to ground, V_N. The voltage difference between needle and extractor is kept fixed. Therefore both the electrospray inside the needle-extractor region, and the electric current in the form of positively charged droplets exiting the extractor, remain unchanged and independent of V_N. When the potential of the needle is well below ground the positive droplets cannot reach the collector and no current is measured in Figure 3. Conversely, for large positive values of V_N the whole current of the electrospray beam is measured at the collector. Main and satellite droplets coexist in this spray: the current associated with the former appears in a range of needle's voltage centered around 301 V, while satellite droplets are observed around 754 V. We will take the value of V_N at one half of the total electric current associated with a given type of droplet as the representative stopping potential, V_S, of that type of droplet. Thus, in Figure 3, we take 301 V and 754 V as the "representative" stopping potentials of main and satellite droplets respectively.

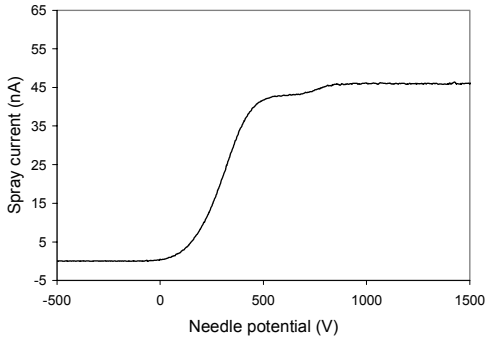

Figure 3 Typical stopping potential curve for an electrospray of solution TBP3

The flow rates with satellite and main droplets are most interesting because the voltage difference between the electrospray needle and the jet's breakup point, as well as the velocity of the jet at this location (v_B), can be inferred when both types of droplets are emitted. To show this, let us recall the expression for the stopping potential of an electrospray droplet[13]

$$V_S = (V_N - V_B) - \frac{1}{2}\frac{m}{q} v_B^2 \qquad [1]$$

where the subscript '*B*' identifies parameters at the breakup point. The term within brackets is the voltage difference between the base of the Taylor cone and the breakup point, a meaningful characteristic very much independent of V_N. m/q stands for the specific charge of the droplets, a parameter that is measured using the time of flight technique. Note that time dependent contributions to the electric field in the proximity of the breakup location are neglected in [1]. We also will consider that the velocity and electric potential of the fluid remain constant upon its detachment from the jet. This approximation is justified because the difference in either voltage or kinetic energy per unit charge between the emerging droplet and the jet must be of the order of the change during the breakup in surface energy per unit charge, $\gamma Q/(R_B I)$, and we will show in following paragraphs that this group is a small quantity compared to either $\frac{1}{2}\frac{m}{q} v_B^2$ or $V_N - V_B$. Furthermore, because main and satellite droplets are generated at the same jet location, we will take the values of $V_N - V_B$ and v_B

associated with both types of droplets to be the same.

Once the specific charge and the stopping potential of a droplet are measured with the time of flight andstopping potential techniques, expression [1] becomes an algebraic equation with two unknowns, V_N-V_B and v_B. Because two independent equations, one for satellites and another for main droplets, can be set, there is sufficient information to determine both V_N-V_B and v_B. We have determined in this way the voltage drop along the cone-jet and the velocity of the fluid at the breakup location for several electrosprays. Table 2 collects the values of the relevant jet parameters for a representative experimental run of each solution. The electrospray flow rate, measured with the bubble flowmeter, and the electric current are given in the second and third columns. They are followed by the specific charge of main and satellite droplets, and their stopping potentials. The values of V_N -V_B and the voltage difference between needle and extractor, V_O, appear in the eighth and ninth columns. V_O is the available voltage for the electrospraying process. The large fraction of V_O spent in accelerating the jet is noteworthy. We will see in the following paragraphs that a fair fraction of this voltage drop is spent reversibly, i.e. the potential drop is mostly transformed in droplet kinetic energy. In fact, the larger the conductivity, the more correct this statement is. The last column collects the velocity of the fluid at the breakup location.

Table 2 Voltage drop and velocity at jet's breakup location, and other relevant parameters of the electrospraying process.

Solution	Q ($m^3 s^{-1}$)	I (nA)	<q/m> main (C kg^{-1})	<q/m> sat. (C kg^{-1})	V_S main (V)	V_S sat. (V)	$V_N - V_B$ (V)	V_O (V)	v_B ($m s^{-1}$)
TBP1	$7.5x10^{-13}$	45	59.1	225.9	110	508	649	1469	252
TBP2	$1.62x10^{-13}$	43	26.9	139.4	143	607	718	1547	176
TBP3	$6.53x10^{-12}$	47	7.0	19.1	301	754	1018	1562	100
TBP4	$2.06x10^{-11}$	45	2.15	6.44	311	810	1060	1766	57
TBP5	$9.56x10^{-11}$	62	0.57	1.84	290	1232	1657	1766	39

We can confirm independently the validity of the experimental values of V_N-V_B and v_B given in Table 2 using the momentum equation for the jet. The following relation is a good approximation for the momentum balance in the reversible section of the jet, downstream the transition region

$$\frac{d}{dx}\left(\frac{\rho v^2}{2} + p\right) = E_t \xi \qquad [2a]$$

where E_t is the tangential electric field acting on the surface of the jet, and ξ is the volumetric charge of the jet. Because in this part of the jet ξ remains approximately constant, [2a] can be integrated to obtain the algebraic equation

$$\frac{\rho v^2}{2} + p + \phi\xi = C \qquad [2b]$$

ϕ is the electric potential and C a constant of integration. Finally, using $Q=\pi R^2 v$ and $I=\xi Q$ Eq. (2b) can be rearranged to yield:

$$[V_N - V(x)] - \Delta = \frac{1}{2}\frac{Q\rho}{I} v(x)^2 + \frac{Q}{I}\left[\frac{\gamma}{R(x)} - \frac{I^2}{8\varepsilon_0 Q^2} R(x)^2\right] \qquad [2c]$$

In this expression we have split the pressure term into its capillary and electric components. The variable "x" stands for a generic position along the jet axis, downstream the transition region. The symbol Δ stands for a constant of integration.

Finally, we can make this equation dimensionless dividing every term by the irreversible voltage loss V^*:

$$V^* = \left(\frac{\gamma^2}{K(\rho\varepsilon_0)^{1/2}}\right)^{1/3} \quad [3]$$

Let us now use the data from Table 2 to check whether they are consistent with the equation of conservation of momentum for the jet. We will compute the right hand side of [2c] using the measurements of Q, I and the radius of the jet at the breakup, and plot this quantity versus V_N - V_B. According to [2c], a linear relation with unity slope between these points is necessary to validate our measurements of V_N -V_B and v_B. We list in Table 3 the voltage drop, inertial, capillary and electric pressure terms at the jet's breakup point associated with the data from Table 2. We have used the characteristic voltage V^*, [3], to make these parameters dimensionless. Note that the kinetic term is much larger than any of the pressure terms. In other words, most of the voltage drop along the reversible part of the jet is spent in accelerating the fluid. It is also clear that the previous statement about $\frac{1}{2}\frac{m}{q}v_B^2$ being much larger than $\gamma Q/(R_B I)$ is also correct. Figure 4 plots the voltage difference between electrospraying needle and breakup point, versus the addition of the three terms in the right hand side of [2c] (again, we point out that V^* is used to make dimensionless these values). We plot the data listed in Table 3 as well as mesurements associated with other electrosprays. The linearity of the data, in such wide range of electrical conductivities and flow rates, is noteworthy. More interesting is the fact that the slope, 0.95, is close to one, as expected. Note that the interception with the ordinate axis, with a value of 16.8, is associated with the irreversible voltage drop in the transition region of the cone-jet, ΔV^*. ΔV^* was previously found to be constant, independent of either the liquid flow rate or electrical conductivity. The good correlation observed in Figure 4 supports the validity of the experimental data in Table 2. Furthermore, numerical and analytical models of the cone-jet should yield solutions for these well defined electro-fluiddynamic parameters. Hence, their comparison with our experimental data for V_N -V_B and v_B will allow the confirmation or rejection of these electrospray theories

Table 3. Jet's breakup parameters required to test [2c]. Notice that the values in 5th to 8th columns are made dimensionless using V^*.

Solution	Q (m^3 s^{-1})	R_B (μm)	$\frac{V_N - V_B}{V^*}$	Kinetic term	Capillary Press.	Electric Pressure
TBP1	7.5×10^{-13}	0.031	90.4	72.7	2.1	0.1
TBP2	1.62×10^{-13}	0.054	73.0	57.5	1.9	0.1
TBP3	6.53×10^{-12}	0.14	59.7	39.8	1.5	0.1
TBP4	2.06×10^{-11}	0.34	42.8	28.7	1.5	0.1
TBP5	9.56×10^{-11}	0.88	50.5	35.6	1.5	0.2

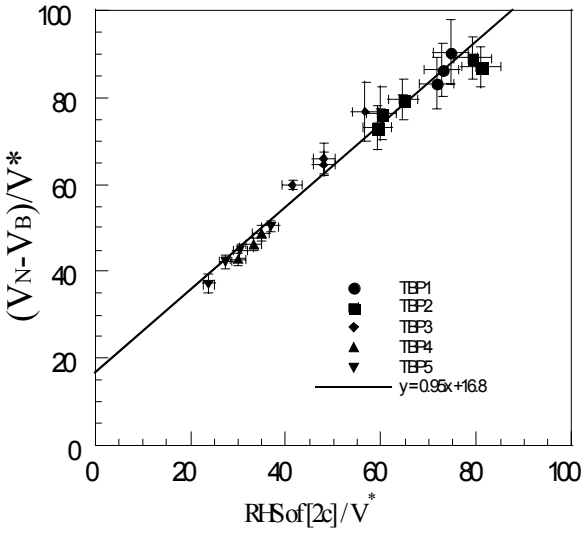

Figure 4. Validation of the measurements of $V_N - V_B$ and v_B using the data in Table III and Eq. [2c].

IV. Conclusions

We have used time of flight and energy analysis techniques to measure the voltage drop and velocity of the jet emerging from a Taylor cone. To the best of our knowledge, this is the first study in which any of these parameters has been experimentally determined in charged jets of submicron radii. A large fraction of the available electrical potential is used to accelerate the charged jet. For the less conducting solutions, the voltage drop between electrospraying needle and jet's breakup point is as much as 90 % of the voltage of the needle. The specific kinetic energy of the fluid at the breakup position is much larger than either the capillary or electric pressures. Our measurements offer a set of well defined electro-fluiddynamic parameters in a wide range of electrospraying conditions. Other researchers working in analytical or numerical calculations of the cone-jet electrospraying mode will find these experimental parameters to be of help in modeling the problem, and ultimately, in confirming or rejecting their models' results. This activity is necessary to improve the current knowledge about Colloid thrusters

Acknowledgements

This research is supported by a NASA Phase II SBIR contract. We acknowledge gratefully the support given by Dr. J. Sovey, the NASA technical monitor of this contract.

1. V. E. Krohn. "Liquid metal droplets for heavy particle propulsion", Progr. In Astronautics and Rocketry, A. C. Press, N. Y. – London, Vol. 5 (1961).
2. V. E. Krohn. "Glycerol droplets for electrostatic propulsion", ARS Electric Propulsion Conference, Berkeley, CA (1962).
3. M. N Huberman & S. G. Rosen. "Advanced high-thrust colloid sources", J. of Spacecraft, 11, 475-480 (1974).
4. M. N.Huberman. "Measurement of the energy dissipated in the electrostatic spraying process", J. Appl. Phys. 41, 578-584 (1970).
5. P. W. Kidd & H. Shelton. "Life test (4350 hrs.) of an advanced colloid thruster module". Paper AIAA 73-1077, AIAA 10th Electric Propulsion Conference, Lake Tahoe, NV (1973).
6. M. Martinez-Sanchez, J. Fernández de la Mora, V. Hruby, M. Gamero-Castaño & V. Khayms. "Research on colloid thrusters", 26th International Electric Propulsion Conference, Kitakyushu, Japan (1999).
7 M. Cloupeau & B Prunet-Foch "Electrostatic spraying of liquids: main functioning mode" J. Electrostat. 25, 165-184 (1990).
8 M. Gamero-Castaño & V. Hruby. "Electrospray as a Source of Nanoparticles for Efficient Colloid Thrusters", J. of Propulsion and Power 17, 977-987 (2001). Also as AIAA Paper 2000-3265 , 36th Joint Propulsion Conference, Huntsville, AL (2000)
9 M. Gamero-Castaño & V. Hruby. "Electric measurements of charged sprays emitted by cone-jets". Submitted to the Journal of Fluid Mechanics (2001).

10 M. Gamero-Castaño, I. Aguirre-de-Carcer, L. de Juan & J. Fernández de la Mora. "On the current emitted by Taylor cone jets of electrolytes in vacuo: implications for liquid metal ion sources", J. Appl. Phys., 83, 2428-2434 (1998).

11 J. A. Riddick, W. B. Bunger & T. K. Sakano "Organic solvents. Physical properties and methods of purification". Wiley, New York, 4th edition (1986).

12 M. Gamero-Castaño & J. Fernández de la Mora. "Direct measurement of ion evaporation kinetics from electrified liquid surfaces". J. Chem. Phys., 113, 815-832 (2000).

13 M. Gamero-Castaño. "The transfer of ions and charged nanoparticles from solution to the gas phase in electrosprays". Ph. D. Thesis, Yale University (1999).